

Domain swapping between FEN-1 and XPG defines regions in XPG that mediate nucleotide excision repair activity and substrate specificity

Marcel Hohl¹, Isabelle Dunand-Sauthier², Lidija Staresinic^{1,3},
Pascale Jaquier-Gubler², Fabrizio Thorel², Mauro Modesti⁴,
Stuart G. Clarkson² and Orlando D. Schärer^{1,3,*}

¹Institute of Molecular Cancer Research, University of Zurich, Switzerland, ²Department of Microbiology and Molecular Medicine, University Medical Centre, Geneva, Switzerland, ³Department of Pharmacological Sciences, SUNY Stony Brook, New York, USA, ⁴Department of Cell Biology and Genetics, Erasmus Medical Center, Rotterdam, The Netherlands

Received August 21, 2006; Revised February 1, 2007; Accepted February 2, 2007

ABSTRACT

FEN-1 and XPG are members of the FEN-1 family of structure-specific nucleases, which share a conserved active site. FEN-1 plays a central role in DNA replication, whereas XPG is involved in nucleotide excision repair (NER). Both FEN-1 and XPG are active on flap structures, but only XPG cleaves bubble substrates. The spacer region of XPG is dispensable for nuclease activity on flap substrates but is required for NER activity and for efficient processing of bubble substrates. Here, we inserted the spacer region of XPG between the nuclease domains of FEN-1 to test whether this domain would be sufficient to confer XPG-like substrate specificity and NER activity on a related nuclease. The resulting FEN-1-XPG hybrid protein is active on flap and, albeit at low levels, on bubble substrates. Like FEN-1, the activity of FEN-1-XPG was stimulated by a double-flap substrate containing a 1-nt 3' flap, whereas XPG does not show this substrate preference. Although no NER activity was detected *in vitro*, the FEN-1-XPG hybrid displays substantial NER activity *in vivo*. Hence, insertion of the XPG spacer region into FEN-1 results in a hybrid protein with biochemical properties reminiscent of both nucleases, including partial NER activity.

INTRODUCTION

FEN-1 and XPG belong to the FEN-1 family of structure-specific nucleases, the members of which fulfill diverse biological roles and cleave branched DNA structures with conserved polarity at the junction of single-stranded (ss) and duplex (ds) DNA (1). FEN-1 has an essential role in DNA replication in the processing of Okazaki fragments and has additional functions in base excision repair and in other pathways contributing to the maintenance of genome stability (2,3). XPG plays a central role in nucleotide excision repair (NER) where it makes the incision on the 3' side of the DNA lesion (4–8). XPG also fulfills a structural role in the assembly of NER complexes since its presence, but not its catalytic activity, is required for the 5' incision by ERCC1-XPF (9–11). Consistent with the contribution of FEN-1 and XPG to different DNA repair and replication pathways, they show similar but distinct substrate specificities *in vitro*. XPG shows structure-specific properties cleaving artificial DNA structures that contain ss/ds DNA junctions, including bubbles and splayed arm substrates with the same polarity as in the NER reaction (7,12,13). In contrast, FEN-1 only acts on substrates that have free 5' ss DNA ends and does not process DNA bubble structures or loops that are substrates for XPG (14,15). In addition, the nuclease activity of FEN-1 is greatly increased on a double-flap structure containing a 1-nt 3' flap adjacent to the 5' flap compared to the conventional 5' flap substrate (16,17).

*To whom correspondence should be addressed. Tel: 631 632 7545; Fax: 631 632 7546; E-mail: orlando@pharm.stonybrook.edu

Present addresses:

Marcel Hohl, Molecular Biology Program, Memorial Sloan-Kettering Cancer Center, 10021 New York, USA; Isabelle Dunand-Sauthier, Department of Pathology and Immunology, University Medical Centre, Geneva, Switzerland; Fabrizio Thorel, Department of Genetic Medicine and Development, University Medical Centre, Geneva, Switzerland

The authors wish it to be known that, in their opinion, the first two authors should be regarded as the joint First Authors.

Such double-flap structures might be the real *in vivo* substrates for FEN-1 during replication (18).

Members of the FEN-1 family of nucleases have a conserved nuclease core composed of the N-terminal (N-) and internal (I-) regions (1). Crystal structures of FEN-1 family proteins from different species revealed that the N- and I- regions form a conserved globular domain containing the active site (19–22). In most FEN-1 family members, the N- and I- regions are separated by <70 amino acids. This region forms a helical arch that is located above the active site and plays a role in DNA binding and catalysis (23). In addition, FEN-1 contains a small surface-exposed hydrophobic wedge and a 1-nt-binding pocket, which provides specificity for double-flap structures and appears to contribute to the positioning of the ssDNA 5' flap near the active site (24,25).

XPG differs from the other FEN-1 family members in that the N- and I- regions are separated by a stretch of over 600 amino acids designated 'spacer region', which shows no homology to other known proteins or motifs (26). An obvious role for this spacer region would be in conferring the substrate specificity and mediating protein–protein interactions required for NER. Indeed, some parts of the spacer region interact with the XPB, XPD, p62 and p44 subunits of the transcription/repair factor TFIIH (27) and perhaps also with RPA (28). The interaction between TFIIH and XPG is of particular relevance since TFIIH needs to be present at sites of DNA damage for the recruitment of XPG following the initial damage recognition by XPC-HR23B (29–31). To address the role of the XPG spacer region, we have generated several mutants of XPG in a previous study and showed that deletions in the spacer region can result in loss of NER activity and defective interaction with TFIIH (32,33). Furthermore, the spacer region of XPG contributes to the substrate specificity of XPG as it is required for efficient bubble cleavage activity. These results demonstrate that the spacer region is, to a significant degree, responsible for the NER-specific functions of XPG.

In the present study, we tested whether the spacer region is sufficient for mediating NER-specific function of XPG or whether additional parts of the protein contribute. For this purpose, we inserted the XPG spacer region between the N- and I- regions of the FEN-1 protein and investigated the biochemical and cell biological properties of this FEN-1-XPG hybrid protein. Our studies reveal that FEN-1-XPG displays specificities on model substrates reminiscent of both XPG and FEN-1, demonstrating that it is a gain of function modification with respect to both XPG and FEN-1. FEN-1-XPG displayed partial NER activity *in vivo*, showing that the insertion of the XPG spacer region in the FEN-1 backbone allows the hybrid protein to carry out NER-related functions.

MATERIALS AND METHODS

Construction of FEN-1-XPG hybrid mutant

To construct *FEN-1-XPG*, *FEN-1* DNA sequence from nucleotide 1 to 315 (fragment I) was amplified by PCR using the primer (5'-AATTCAATCAGCGCCGCAT

GGAATTCAAGGCCTGGC) and (5'-AATTCAAAGCTCCGCCGCTCACTGCGTTTG) and the plasmid pET28a-*FEN-1* as template. The primers incorporated a NotI restriction site 5' of the *FEN-1* ORF and a HindIII restriction site 3' of the PCR fragment. Primers (5'-AATTCAATCAATTAATGCTGAGGCAGAGAAGCAGG) and (5'-AATTCAGGTACCTTAATGATGGTGTGATGGTGTTCCTTTTAAACTTCCC) were used to amplify the *FEN-1* sequence from nucleotide 316 to 1143 (fragment II), introducing a 5' AseI restriction site, a His6 tag and the stop codon followed by a KpnI restriction site at the 3' end. pFastBac1-*XPG* (13) was digested with NotI and AseI, and the 2.2 kb NotI-AseI *XPG* fragment was ligated together with the AseI-KpnI digested *FEN-1* fragment II and the NotI-KpnI digested pFastBac1 vector in a three-point ligation. The NotI-HindIII digested *FEN-1* fragment I was ligated into the NotI-HindIII digested pFastBac1 vector.

For transduction of XP-G/CS fibroblasts, *FEN-1-XPG* (in pFastBac1) and *FEN-1* (in pET28a) cDNA constructs were cloned into the pLOX/EWgfp lentiviral vector by replacing the *GFP* cDNA (32).

XPG, FEN-1 and FEN-1-XPG hybrid proteins expression and purification

XPG and FEN-1-XPG were expressed in Sf9 insect cells and purified as described previously (13), with minor modifications. The majority of XPG and FEN-1-XPG eluted from the nickel beads at 100 mM imidazole. XPG eluted from the HiTrap S column between 400 and 600 mM NaCl and FEN-1-XPG between 350 and 500 mM NaCl. From the HiTrap Q column, XPG eluted between 450 and 600 mM NaCl and FEN-1-XPG between 500 and 650 mM NaCl. Protein concentrations were determined using the Bradford protein assay with BSA as a standard. Concentrations between 0.1 and 0.3 mg/ml of purified proteins were obtained with an overall yield of 0.2–0.5 mg.

Human *FEN-1* cDNA was amplified by PCR from HeLa RNA first-strand cDNA synthesis (Clontech), equipped with a C-terminal His6 tag and cloned into pET28a using NcoI and XhoI restriction sites. The plasmid was transformed into the Rosetta pLysS strain (Novagen) and grown at 37°C to an OD_{600nm} of 0.6 and induced with 1 mM IPTG for 4–5 h at 37°C. The cells were lysed by sonication in buffer A (500 mM NaCl, 20 mM Hepes pH 8, 10% glycerol, 2 mM β-mercaptoethanol, 0.1% NP-40) and batch purified over Ni-NTA Sepharose using buffer A + 2 mM imidazole for loading and eluted with buffer A + 60 mM imidazole. Fractions containing FEN-1 were dialyzed against buffer Z (20 mM Hepes pH 8, 10% glycerol, 2 mM DTT, 1 mM EDTA) + 50 mM KCl and purified on a S Sepharose column using a gradient of 50 mM to 1 M KCl. FEN-1 eluted as a sharp peak at around 400 mM KCl.

DNA binding and cleavage and *in vitro* NER assays

Oligonucleotides described previously (see Table 1 in (13)) were used to generate the splayed arm (oligonucleotide A₂₀ and B₁₉), flap (oligonucleotide A₂₀, B₁₉ and C₁₉) and bubble substrates. DNA cleavage and binding assays were

performed as described previously (13). To construct the double-flap substrate containing a 1-nt 3' flap, oligonucleotide C₂₀ that contains one additional A nucleotide at the 3' end was used instead of oligonucleotide C₁₉. Substrates were annealed with a 2-fold excess of the unlabeled oligonucleotide(s). In DNA cleavage assays, the reaction was activated by addition of 0.5 mM MnCl₂ for XPG and 1 mM MnCl₂ for FEN-1 and FEN-1-XPG. Cleavage assays were analyzed by denaturing and binding assays by native PAGE. Each gel was quantified using a Typhoon 9400 PhosphorImager (Amersham Biosciences) and Image Quant version 5.2 software from Molecular Dynamics. In all studies, the amount of substrate and product was quantified, and the percentage of substrate cleavage was determined by the product/(substrate+ product) ratio. This method allows for correction of any loading errors among lanes. All assays were performed at least in duplicate, and representative gels are shown.

For the *in vitro* NER assay, a 24-mer oligonucleotide containing a unique GTG sequence (5'-TCTTCTTCTGTGCACTCTTCTTCT) was platinated to produce a 1,3-intrastrand GpTpG-crosslink. This oligonucleotide was used in primer extension reaction with ssDNA of pBluescript KS⁻ as a template, and purified as described previously (34). The NER assay was performed as described previously (32).

Cell culture conditions, preparation of whole-cell extracts and transduction with lentiviral recombinants

For the generation of whole-cell extracts, SV40 transformed fibroblasts XPCSIRO (35) were cultured in Modified Eagle's Medium (MEM) (Gibco) supplemented with 10% fetal calf serum (FCS) and 2 mM L-glutamine, 100 U/ml penicillin and 100 mg/ml streptomycin at 37°C in the presence of 5% CO₂. Cells were grown to near confluency, and whole-cell extract was prepared according to a published procedure (36).

For the transduction experiments, primary fibroblasts from a severely affected XP-G/CS patient (XP20BE) (37,38) were cultured in MEM supplemented with 15% FCS, 2 mM L-glutamine, 100 U/ml penicillin and 0.1 mg/ml streptomycin. Cells were grown in a 5% CO₂ humidified incubator. 293T cells were cultured in Dubelcco Modified Eagles Medium (DMEM) supplemented with 10% FCS, 2 mM L-glutamine, 100 U/ml penicillin and 0.1 mg/ml streptomycin and kept in a 5% CO₂ humidified incubator. Recombinant lentiviruses containing the XPG, FEN-1-XPG and FEN-1 cDNAs under the control of the EF1 α promoter were produced as described previously (32). Infection was carried out by adding the viral particles containing the different recombinants to XP-G/CS primary fibroblasts (XP20BE) at 50% confluency. Fibroblasts were then cultured normally for various times, and the transduction efficiency was assessed by immunofluorescence and western blotting.

Survival assay and detection of 6-4 photoproducts by immunodot blot analysis

Cells were irradiated as described previously (32), and viability was assessed 72 h post-irradiation using the

CellTiter 96 AQueous One Solution Cell Proliferation Assay (Promega) according to the manufacturer's instructions. The number of proliferating cells was measured by recording the absorbance at 490 nm with a 96-well plate reader (Bio-Rad). Viability assays were performed independently four times using three independent sets of transduced cells. For immunodot blots, cells were irradiated with a UVC dose of 20 J/m² and pelleted at different times post-UV. DNA was isolated using the Puregene method (Gentra systems) according to the manufacturer's instructions. Immunodot blots were performed as previously described (39) using 64M-2 antibodies against 6-4PPs (gift from O. Nikaido).

Local UV irradiation and immunofluorescence

Local UV irradiation and immunofluorescence were performed as described previously (32) with the following modifications. The primary antibodies, mouse monoclonal anti-XPG (clone 1G12, gift from J.M. Egly) at 1/1000 dilution and rabbit polyclonal anti-p89 at 1/600, were added for 1 h at room temperature in 1 \times PBS containing 1% BSA. Detection of 6-4PPs was performed as described previously. Transduced cells were analyzed for the presence/absence of foci, and untransduced cells were used as negative control. Stained cells were observed in a Zeiss AxioCam microscope using the Axiovision software.

RESULTS

Construction and purification of FEN-1-XPG hybrid protein

In a previous study, we have shown that the deletion of the spacer region in XPG resulted in a defect in NER and in reduced bubble cleavage activity (32). We wanted to test whether the spacer region is sufficient to mediate these XPG-specific functions and reasoned that the insertion of the 600 amino acid spacer region of XPG into the homologous FEN-1 protein would be a suitable experimental approach to test this notion. FEN-1 shares a conserved nuclease domain (N- and I- regions) with XPG, but its N- and I- regions are separated by only about 70 amino acids, defined as a helical clamp structural motif. Based on FEN-1 crystal structures (21,22), we hypothesized that the insertion of XPG spacer into FEN-1 between amino acid residue 104 and 105, in an unstructured region just N-terminal to α helix 4, should not dramatically alter the structure of the FEN-1 nuclease active site. We incorporated new HindIII and AseI restriction sites into FEN-1 by PCR and inserted the XPG DNA fragment corresponding to the XPG spacer region from amino acid residue 108 to 732 (Figure 1A), as described in the 'Materials and methods' section. We refer to this hybrid protein as FEN-1-XPG.

XPG and FEN-1-XPG protein with a C-terminal his tag were expressed in Sf9 insect cells and purified as described previously (13) (Figure 1B). The FEN-1-XPG protein of 1005 amino acids was soluble and presented similar elution profiles to XPG during protein purification, indicating that the hybrid protein is properly folded. Since the spacer region of XPG is very acidic (pI 4.5), its insertion into FEN-1 yielded a hybrid protein with

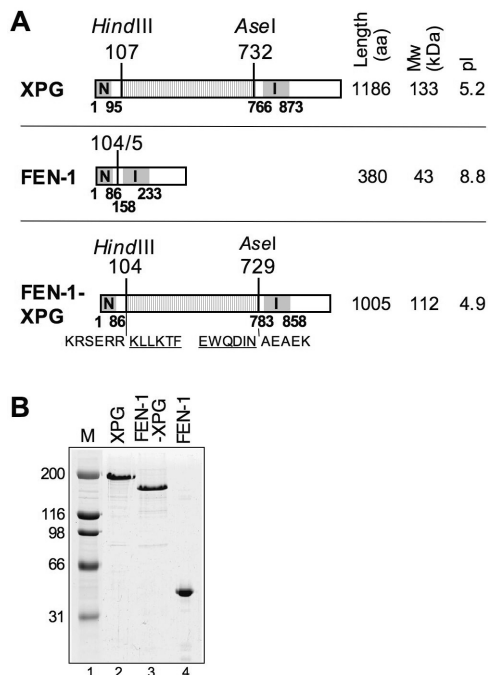


Figure 1. Construction and purification of FEN-1-XPG hybrid protein. (A) Schematic representation of XPG, FEN-1 and FEN-1-XPG hybrid proteins. The conserved N- and I- nuclease regions are indicated. The HindIII and AseI restrictions sites were incorporated by site-directed mutagenesis into FEN-1 at amino acids position 104/105. These sites were used to insert the HindIII-AseI fragment of the XPG spacer (residues 108 to 732) into FEN-1 to generate the FEN-1-XPG hybrid. The amino acid sequences at the cloning sites are shown. The number of amino acids (aa), the molecular weight (Mw) and the isoelectric point (pI) values of the proteins are indicated. (B) XPG and FEN-1-XPG were expressed and purified from Sf9 insect cells, and FEN-1 was purified from *Escherichia coli* as described in the 'Materials and methods' section. Purified proteins were analyzed on an 8% SDS-polyacrylamide gel. Lane 1, broad range marker (1 μ g of protein/band); molecular weights are indicated. Lane 2-4, 2 μ g of XPG, FEN-1-XPG and FEN-1 proteins, respectively.

significantly lower pI of 4.9 compared to FEN-1 (pI of 8.8). As observed for XPG, the FEN-1-XPG hybrid protein of 112 kDa migrated above its molecular weight on SDS-PAGE (Figure 1B), providing further evidence that the low pI of the spacer region is responsible for the abnormal migration behavior of XPG (32).

FEN-1-XPG exhibits endonuclease activity on flap and bubble substrates

We first wanted to examine whether the insertion of the 600 amino acids spacer of XPG into FEN-1 protein has any effect on the proper folding of the FEN-1 nuclease domain. We performed nuclease assays with increasing concentrations of purified XPG, FEN-1-XPG and FEN-1 on a flap substrate, which is processed by both XPG and FEN-1 (12,40). FEN-1-XPG showed comparable activity to XPG on the flap substrate in the presence of either Mg^{2+} or Mn^{2+} (Figure 2A, compare top and middle panel, Figure 2C, left panel and data not shown). This result confirms that the insertion of the 600 amino acid spacer region into FEN-1 does not interfere with the

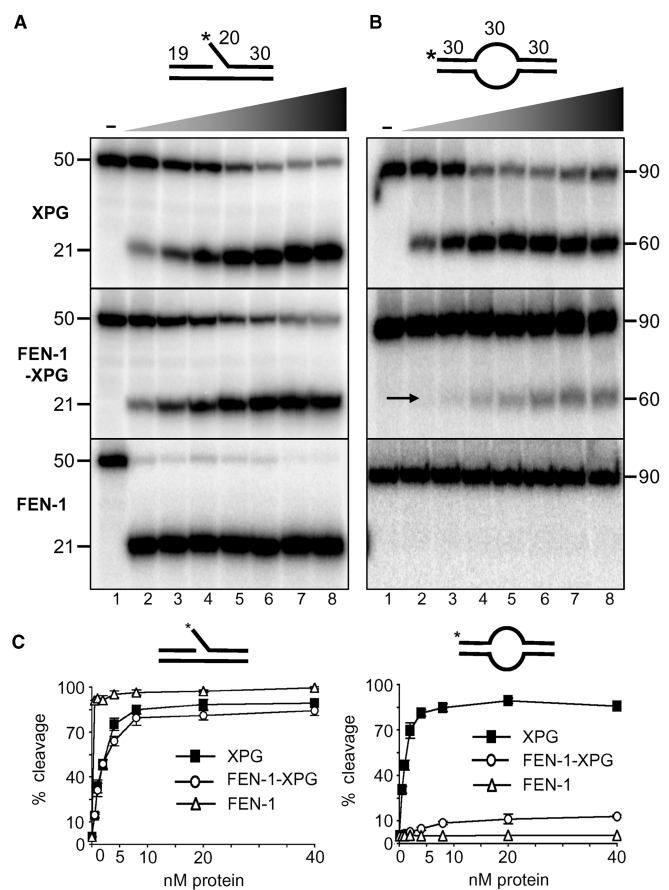


Figure 2. Endonuclease activity of FEN-1-XPG hybrid protein on flap and bubble substrates. (A) Purified proteins were incubated for 45 min at 30°C with 2.5 nM of flap substrate (lanes 1-8) in the presence of 0.5 mM $MnCl_2$ for XPG and 1 mM $MnCl_2$ for FEN-1-XPG and FEN-1. The following protein concentrations were used: 0 nM (lane 1), 0.5 nM (lane 2), 1 nM (lane 3), 2 nM (lane 4), 4 nM (lane 5), 8 nM (lane 6), 20 nM (lane 7) and 40 nM (lane 8). The position of the $5^{32}P$ label on the substrate is indicated by the asterisk. The length of the products was determined by comparison with an authentic standard and is indicated. (B) Incision activity of purified proteins on the bubble substrate using the conditions described in A. (C) Cleavage efficiency of XPG, FEN-1 and FEN-1-XPG on the flap substrate (left) and bubble substrate (right) with increasing protein concentration. Graphs represent the quantification of two independent experiments. Standard deviations are represented by error bars.

proper folding of the nuclease domain. However, the hybrid protein showed somewhat reduced nuclease activity compared to FEN-1 (Figure 2A, compare middle and bottom panel; Figure 2C, left panel). It has been previously shown that the flexible loop between the nuclease domains in FEN-1 assumes an ordered conformation upon substrate binding, which might be important for efficient cleavage by properly positioning the substrate (22,41). It is likely that the insertion of the spacer region in the flexible loop interferes with a structural rearrangement, resulting in reduced activity of FEN-1-XPG compared to FEN-1.

XPG exhibits nuclease activity on bubble substrates, while FEN-1 is unable to cleave such substrates (14,15,40). Since the XPG spacer region was shown to be essential for

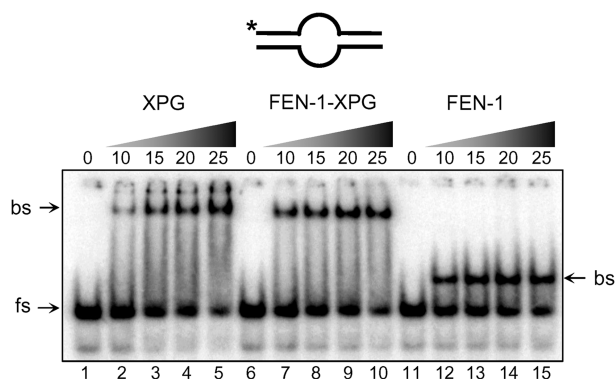


Figure 3. DNA binding of XPG, FEN1-XPG hybrid and FEN1 proteins to bubble substrates. DNA binding was analyzed using electrophoretic mobility shift assays. Radiolabeled bubble substrate (2.5 nM) was incubated in nuclease buffer A for 15 min in the presence of a 50-fold excess of cold dsDNA competitor in the absence of divalent metal ions with increasing concentrations of XPG (lanes 2–5), FEN1-XPG (lanes 7–10), FEN1 (lanes 12–15) or no protein (lanes 1, 6 and 11). The following protein concentrations were used: 10 nM (lanes 2, 7 and 12), 15 nM (lanes 3, 8 and 13), 20 nM (lanes 4, 9 and 14) and 25 nM (lanes 5, 10 and 15). Bound substrates (bs) were separated from the free or unbound substrate (fs) on a 5% native polyacrylamide gel.

efficient bubble cleavage activity (32), we tested whether FEN1-XPG displayed bubble cleavage activity. As expected, XPG efficiently cleaved the bubble substrate, whereas FEN1 did not (Figure 2B, top and bottom panel, Figure 2C, right panel). FEN1-XPG showed significant activity on the bubble compared to FEN1 (Figure 2B, compare middle and bottom panels), albeit at much lower levels than XPG (Figure 2B, top panel). FEN1-XPG cleavage activity reached a plateau at 10% conversion (Figure 2C, right panel), and longer incubation times did not lead to significantly higher activity (data not shown).

The failure of FEN1 and the low activity of FEN1-XPG to cleave the bubble substrate were not caused by a reduction in DNA substrate binding. Electrophoretic mobility shift assays revealed no significant differences in the binding efficiencies of XPG, FEN1-XPG and FEN1 to a bubble substrate in the presence of a 50-fold excess of cold duplex competitor DNA, demonstrating specific binding to ss/dsDNA junctions (Figure 3).

FEN1 and FEN1-XPG but not XPG show a preference for double-flap substrates

FEN1 was shown to exhibit higher nuclease activity on a double-flap substrate with a 1-nt 3' flap overhang in addition to the 5' flap due to higher substrate-binding activity (16,17,42). Structural studies revealed a specific 1-nt-binding pocket in the N-region explaining this preference for the 3' flap (24). We compared the cleavage activity of XPG, FEN1-XPG and FEN1 on a double-flap substrate with a 1-nt 3' flap. XPG showed equal activity on the single- and double-flap substrates (Figure 4A, compare lanes 2–7 and 9–14), whereas FEN1 had higher nuclease activity on the double flap substrate (Figure 4C, compare lanes 2–7 and 9–14). Like FEN1, the cleavage activity of FEN1-XPG was strongly stimulated

by the presence of the 1-nt 3' flap (Figure 4B, compare lanes 2–7 and 9–14). Although the overall activity of FEN1-XPG was lower than that of FEN1, the degree of stimulation of a double-flap compared to a single-flap substrate was similar for both proteins (Figure 4C). This suggests that the insertion of the spacer region of XPG into the helical loop of FEN1 has no influence on the structure of the 3' 1-nt flap binding pocket. Consistent with this observed preference for cleaving double-flap substrates, FEN1 and FEN1-XPG, but not XPG, showed increased binding activity for the double-flap compared to the single-flap substrate (Figure 5).

FEN1-XPG has partial NER activity *in vivo*

The spacer region of XPG is necessary to mediate protein–protein interactions required for NER (32). We wondered whether the spacer region would be sufficient for NER activity characteristic of XPG when imbedded in a different structure-specific nuclease. We first tested whether the FEN1-XPG hybrid protein could perform the incision 3' to the lesion in an *in vitro* NER assay. We monitored the excision of a 24–32 mer oligonucleotide from a plasmid containing a site-specific 1,3 cisplatin adduct using an extract from a repair-deficient XP-G/CS fibroblast cell line supplemented with recombinant proteins. As expected, the formation of NER excision products was observed upon addition of purified XPG. In contrast, no excision products were detected in the reactions containing FEN1-XPG or FEN1 (Figure 6), even at elevated protein concentrations (data not shown). These results suggest that the spacer region of XPG embedded in FEN1 is not sufficient to support NER incision activity under the conditions used in our *in vitro* assays.

We then tested whether the FEN1-XPG protein was able to correct the UV sensitivity of XPG-deficient cells. We had previously observed that the amount of UV resistance conferred by mutant XPG proteins to XP-G/CS cells was a more sensitive measure of NER activity than the *in vitro* NER assays (32). Primary XP-G/CS fibroblasts (XP20BE) were, therefore, transduced with lentiviral recombinants containing XPG, FEN1 or FEN1-XPG. Transduced cells were irradiated with increasing UV doses (0–6 J/m²), and cell viability was measured using a colorimetric assay at 72 h post treatment. Untransduced XP-G/CS cells lacking a functional XPG protein showed a strong sensitivity to UV irradiation (Figure 7A). Similar UV sensitivity was observed when cells were transduced with a lentivirus containing the *GFP* gene (data not shown). In contrast, when XP-G/CS cells were transduced with XPG, they became resistant to UV irradiation, and more than 80% of these cells survived a UV dose of 6 J/m² (Figure 7A). Surprisingly, we observed an intermediate resistance to UV of transductants expressing FEN1-XPG (Figure 7A). Although no NER activity *in vitro* was observed for FEN1-XPG, it seems that these cells still retain some repair activity *in vivo* and are able to confer some UV resistance. This is not due to an unanticipated activity of FEN1 because control transductants

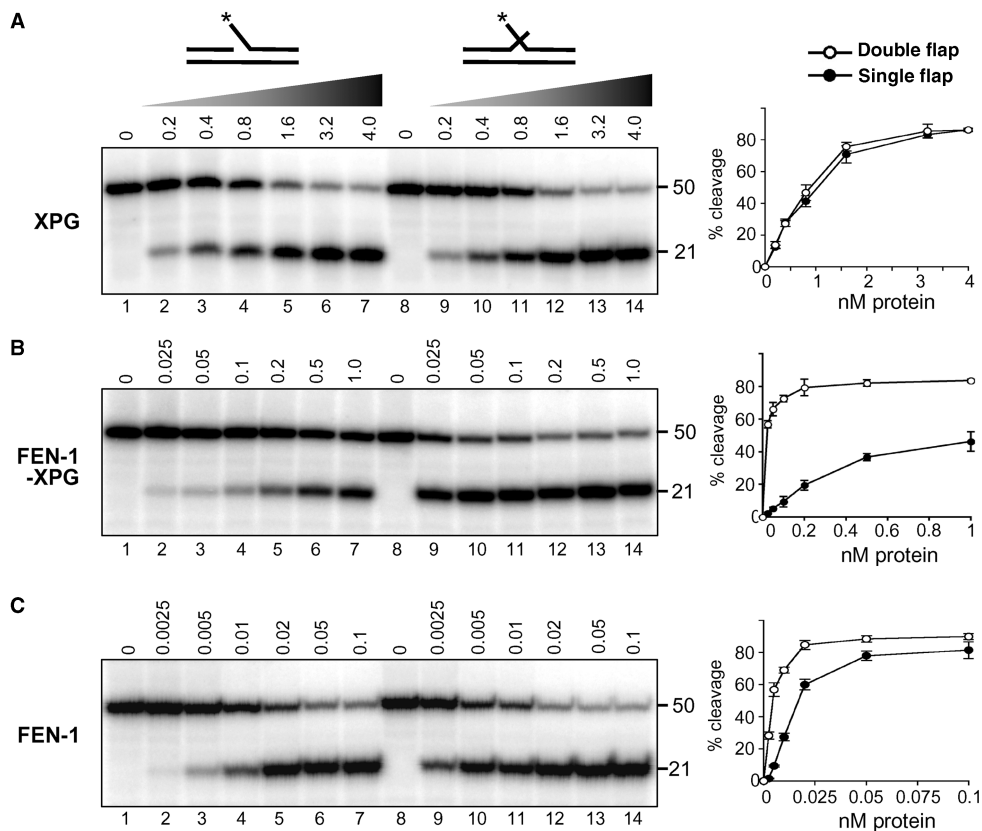


Figure 4. Endonuclease activity of XPG, FEN-1 and FEN-1-XPG on a single- and double-flap substrate. The endonuclease activity of XPG (A), FEN-1-XPG (B) and FEN-1 (C) was assessed on a single 5' flap substrate (lanes 1–7) or on a double-flap substrate with an additional 1-nt 3' flap (lanes 8–14). 2.5 nM of substrate was incubated for 40 min at 30°C in the presence of 0.5 mM MnCl₂ for XPG or 1 mM MnCl₂ for FEN-1-XPG and FEN-1. The different protein concentrations for XPG, FEN1-XPG and FEN-1 are indicated (in nM) on the top of each gel. The position of the 5'³²P label on the substrate is indicated by the asterisk. The length of the products was determined by comparison with authentic standards and is indicated. The percentage of substrate cleavage versus protein concentration is presented graphically (right panels) for each protein. Graphs show the quantification of two independent experiments. Standard deviations are indicated by error bars.

expressing only FEN-1 were as highly sensitive to UV as untransduced XP-G/CS cells (Figure 7A).

To more directly assay DNA repair, we monitored the disappearance of 6-4PPs over time by immunodot blot analysis. XPG, FEN-1-XPG or FEN-1 transductants were exposed to a UV dose of 20 J/m², and genomic DNA was isolated at various times thereafter. The DNA samples were then probed with monoclonal antibodies against the 6-4PPs (43,44). The disappearance of the signals for 6-4PPs over time indicates proper removal of these lesions by NER. As expected for NER-deficient cells, the signals for 6-4PPs persisted up to 48 h post-UV in untransduced XP-G/CS cells (Figure 7B, lane 1, and data not shown). In contrast, these damages were rapidly repaired in XP-G/CS cells expressing XPG (Figure 7B, lane 2). Only background levels of the signal were observed 2–4 h post-UV in XPG/CS cells expressing XPG (Figure 7B, lane 2), indicating that the presence of functional XPG protein renders these cells NER proficient. In transductants expressing FEN-1-XPG, the 6-4PPs signal levels started to decrease at 8 h post-UV and almost disappeared after 24 h (Figure 7B, lane 3). The disappearance of the 6-4PP signal in these transductants suggests that they possess a significantly increased repair activity compared to

untransduced XP-G/CS cells. In contrast, no repair of the 6-4PPs was observed in XP-G/CS cells transduced with FEN-1 (Figure 7B, lane 4). These results are fully consistent with the *in vivo* survival curves (Figure 7A). Together, they suggest that the presence of the XPG spacer region in the FEN-1 backbone modifies FEN-1 nuclease activity to permit the cleavage of UV lesions with significant efficiency, thereby conferring intermediate UV resistance to the FEN-1-XPG transductants.

The FEN-1-XPG hybrid protein is not visible at sites of UV damage

The kinetics of the NER reaction and the assembly and disassembly of the proteins involved at sites of UV damage can be monitored by local irradiation of individual cells and staining of cells at various time points after that using antibodies against UV-damaged DNA or NER proteins (29,45). We have previously used this technique to show that an intact spacer region in XPG is required for the efficient recruitment of the protein to the sites of UV damage (32). Here, we asked whether the presence of the XPG spacer region in the FEN-1 protein would be sufficient to allow the recruitment of the hybrid

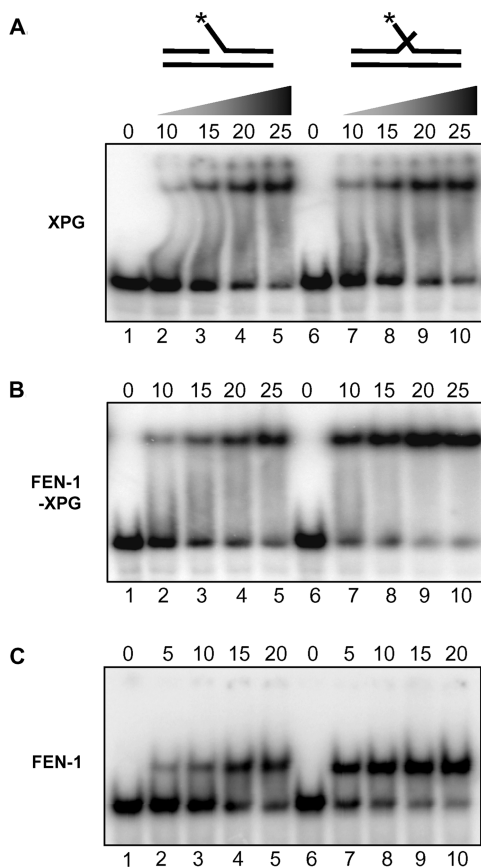


Figure 5. Binding efficiencies of XPG, FEN1-XPG and FEN1 towards a single- and a double-flap substrate. DNA binding was analyzed using electrophoretic mobility shift assays on the same substrates as used in Figure 4. Either 2.5 nM single 5' flap substrate (lanes 1–5) or double-flap substrate with a 1-nt 3' flap (lanes 6–10) was incubated with increasing protein concentrations of XPG (A), FEN1-XPG (B) or FEN1 (C) in the absence of divalent metal ions in nuclease buffer A. The protein concentrations used are indicated (in nM) on the top of each gel.

protein to sites of UV damage. XP-G/CS transductants expressing XPG or FEN1-XPG were irradiated with 150 J/m^2 through an $8 \mu\text{m}$ pore filter. Cells were then fixed 30 min and 24 h post-UV, and the XPG and XPB proteins as well as the 6-4PPs were detected with appropriate antibodies. As shown previously (32), untransduced XP-G/CS cells contain no detectable XPG protein, but the XPB subunit of TFIIH colocalizes with 6-4PPs 30 min post-UV independently of XPG (Figure 8, 30 min post-UV, Untransduced), and these XPB/6-4PPs foci persist for over 24 h (Figure 8, 24 h post-UV, XPB/6-4PPs). Hence, XPG is not needed for the earliest damage recognition events but it is required for damage resolution. In XP-G/CS transductants expressing wild-type XPG, this protein was present in nuclear foci at the UV lesions and colocalized with the XPB and 6-4PPs 30 min post-UV (Figure 8, 30 min post-UV, XPG). By 24 h post-UV, foci for XPG, XPB and 6-4PPs have all disappeared, indicating that repair had been completed (Figure 8, 24 h post-UV, XPG).

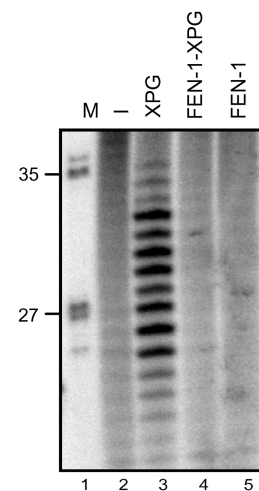


Figure 6. FEN1-XPG does not restore NER activity in an XPG-deficient cell extract. Cell extracts prepared from XPCS1R0 fibroblasts were incubated with a plasmid containing a single 1, 3 cisplatin adduct in absence of protein (lane 2) or in presence of 15 nM purified recombinant XPG (lane 3), FEN1-XPG (lane 4) or FEN1 (lane 5). The excision products containing the cisplatin adduct were labeled by the annealing of an oligonucleotide complementary to the excised oligonucleotides with a 5' GGGG overhang and filling in with $\alpha\text{-}^{32}\text{PdCTP}$ and Sequenase enzyme. The products were separated on a 14% denaturing polyacrylamide gel and visualized by autoradiography. A MspI digest of pBR322 (lane 1) served as size marker.

In the hybrid transductants, FEN1-XPG protein was not detectable in foci that contained XPB and 6-4PPs 30 min post-UV (Figure 8, 30 min post-UV, FEN1-XPG). However, the XPB/6-4PP foci had disappeared by 24 h post-UV, indicating that NER had been completed in these cells (Figure 8, 24 h post-UV, FEN1-XPG). We had previously observed similar results for certain XPG mutants with deletions in the spacer region (32). This behavior of XP-G/CS cells expressing the FEN1-XPG hybrid protein is consistent with the intermediate survival and repair kinetics of these cells. As a possible mechanistic explanation, the FEN1-XPG protein may be recruited less stably or with slower kinetics to NER repair complexes.

DISCUSSION

In this study, we have generated a hybrid human protein containing the nuclease domains of FEN1 and the spacer region of the XPG protein to ask if the spacer region of XPG is sufficient to confer NER-specific functions to a different nuclease scaffold.

Biochemical activities of the FEN1-XPG protein

The FEN1-XPG protein displayed biochemical activities that are characteristic of both XPG and FEN1. Namely, FEN1-XPG was able to cleave bubble substrates, which

are not processed by FEN-1. At the same time, FEN-1-XPG showed a preference for double-flap over single-flap substrates, similar to FEN-1, while the activity of XPG is equal for single or double flaps. We found that the preference for double flaps was a result of increased binding, consistent with the presence of a defined 1-nt-binding pocket in FEN-1 revealed by structural studies (24). Our studies suggest that this binding pocket acts independently of the events surrounding catalysis. The basis for the preferential cleavage of bubbles by XPG

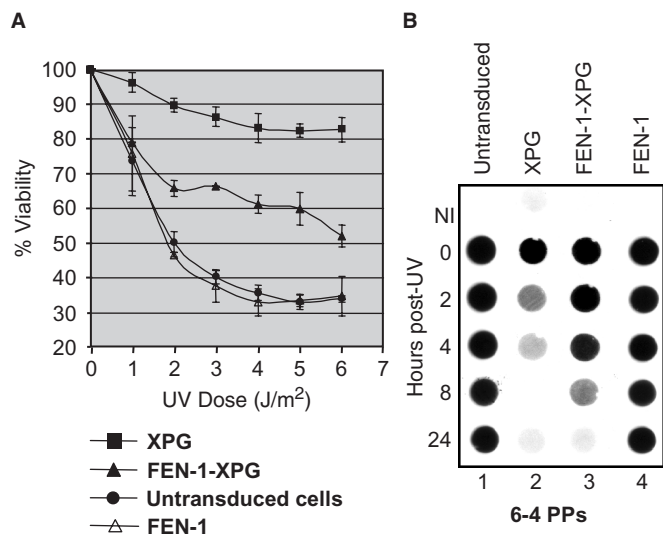


Figure 7. UV damage repair of XP-G/CS transductants expressing the FEN-1-XPG hybrid. (A) UV survival curves of XP-G/CS cells expressing XPG, FEN-1 and FEN-1-XPG proteins. XP-G/CS fibroblasts (XP20BE) were transduced with the indicated cDNAs in lentiviral recombinants and irradiated with the indicated doses of UVC light. Their survival was monitored 72 h later by a colorimetric assay. Each point represents the average of four independent experiments. Error bars indicate the standard errors of the means. (B) Levels of unrepaired UV DNA damage in XP-G/CS cells transduced with *XPG*, *FEN-1-XPG* and *FEN-1* cDNA. Cells were irradiated with a UVC dose of 20 J/m², and the subsequent retention of 6-4PPs was analyzed by immunodot blotting with antibodies against 6-4PPs. NI, non-irradiated.

and FEN-1-XPG over FEN-1 is less straightforward. Our binding studies revealed that XPG and FEN-1-XPG bind bubble substrates with comparable affinities to FEN-1. Similarly, we have previously shown that the change in substrate specificity in XPG proteins with deletion in the spacer region is not due to initial binding events (32). We attempted to express the spacer region separately, but were unable to obtain any soluble protein of that region using a variety of conditions in the bacterial or baculovirus expression systems (data not shown). Furthermore, we were unable to detect this XPG fragment in living cells by immunofluorescence after transduction of a lentiviral construct expressing the spacer region into XPG/CS cells (data not shown). The predicted high degree of disorder in that region is likely responsible for our failure to analyze its properties directly. Although one study has suggested a role for the spacer region in substrate binding and recognition based on the inhibition of the DNA-binding activity of XPG using a monoclonal antibody directed against the spacer region (46), we believe that a prominent role for the spacer region in the catalytic step is most consistent with other available data. For example, it has previously been found that the flexible loop between the nuclease domains in FEN-1 undergoes a rearrangement to facilitate catalysis during the incision reaction (22,41). The fact that FEN-1-XPG, in which this flexible loop has been disrupted by the introduction of the XPG spacer region, shows reduced cleavage activity of flap substrates compared to FEN-1 supports an important role of this loop in catalysis. Our studies suggest that this rearrangement occurs subsequent to initial binding and does not influence the binding affinity. This mechanism of initial binding and subsequent rearrangement to a catalytically active conformation seems to be shared by XPG, as we have previously demonstrated that it displays distinct requirement for binding and catalysis (13).

The low level of bubble cleavage activity of FEN-1-XPG indicates that additional regions of XPG contribute to efficient cleavage activity. Consistent with this, XPG with a deletion in the spacer region showed reduced, but substantial bubble cleavage activity (32). It is, therefore, possible that the N- and I- regions of XPG make

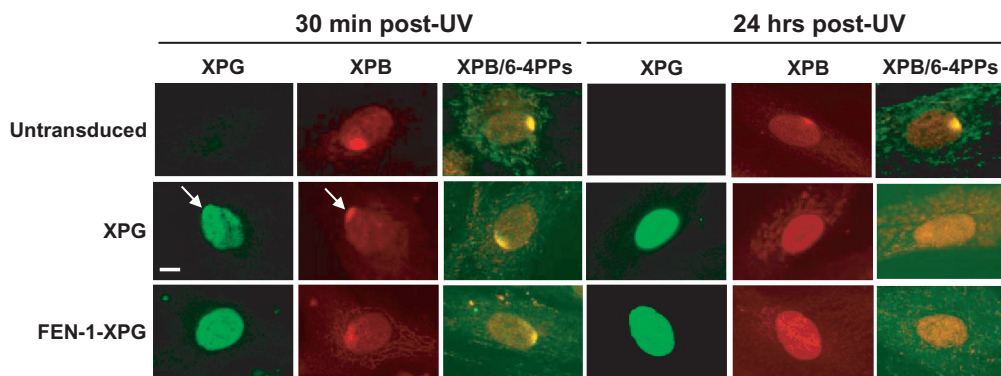


Figure 8. Recruitment of FEN-1-XPG hybrid to local UV sites of damage in XP-G/CS cells. Cells were irradiated at 150 J/m² through a filter with 8 μm pores and fixed 30 min or 24 h after irradiation. Cells were then immunolabelled with antibodies against XPG (green), against the XPB subunit of TFIIH (red) and against 6-4PPs (green). Merged images indicate the overlay of 6-4PPs and XPB staining. Scale bars, 10 μm.

contributions to its unique substrate specificity that set it apart from other FEN-1 family members. Alternatively, the fact that the spacer region is slightly shortened in FEN-1-XPG compared to XPG (it lacks 11 amino acids immediately following the N-region and 33 amino acids prior to the I-region) might limit its proficiency in cleaving bubble substrates.

Recruitment of XPG to NER preincision complexes by TFIIH

The recruitment of NER proteins to sites of repair can readily be investigated using local UV irradiation of nuclei of living cells through polycarbonate filters and subsequent detection of the lesions induced and NER proteins recruited to them by immunohistochemistry (29,45,47). We used this method to evaluate regions in XPG that might contribute to the proper recruitment of the protein to sites of NER. XPG is recruited within 30 min following irradiation, and it depends on the prior recruitment of XPC/HR23B and TFIIH. Twenty-four hours after irradiation, NER proteins are no longer visible in foci, indicating that repair has been completed (32,33). Mutations in the spacer region of XPG can affect recruitment in two ways; in one case, XPG is recruited to UV-damaged sites with normal kinetics, but is then unable to properly execute its function in NER due to unstable association with the preincision complex (33). In the second case, the recruitment of XPG to UV-damaged sites cannot be directly observed. However, since the damage is ultimately repaired, albeit with slower kinetics than in the wild-type situation, it can be inferred that XPG was at some point present at the damaged site (32). The fact that defects in the interaction with TFIIH caused by different mutations in XPG can influence the recruitment of XPG as well as the subsequent processing of NER substrates is a testimony to the complexity of the interaction between the two proteins.

Several years ago, it was suggested that sequences within and downstream of the I-region are also involved in mediating the interaction with TFIIH and hence contribute to the recruitment of XPG to sites of NER (27). Indeed, in ongoing work, we have observed that replacing the C-terminus of FEN-1 in FEN-1-XPG with the C-terminus of XPG yielded a protein that displayed wild-type levels of recruitment to sites of UV damage (data not shown). While the first generation design of this hybrid protein containing the FEN-1 nuclease core and spacer and C-terminal regions of XPG appeared not to result in a fully functional protein and only restored UV resistance to XP-G/CS cells at levels comparable to the FEN-1-XPG protein, it provides evidence that two independent regions in XPG are responsible for the recruitment of the protein to NER preincision complexes by interaction with TFIIH (27,29,30).

Multiple weak interaction sites facilitate progression through the NER pathway

NER is a highly dynamic process that acts by sequential assembly of the factors involved at the site of damage (4,31,48). To ensure progression through the pathway, it is advantageous to employ multiple weak interactions

between the proteins and DNA intermediates involved rather than strong specific interactions such as those employed by transcription factors binding to their DNA substrates (49). The transient nature of many of the interactions involved could serve as a basis for the NER machinery to assemble dynamically and pass on substrates from one subcomplex to the next. The modular structure of the XPG protein and the modular nature of its interaction with TFIIH and DNA fit perfectly within that paradigm. At least two regions of XPG, the spacer region and the C-terminus, interact with the p44, p62, XPD and XPB subunits of TFIIH (27). Recent studies have shown that the first 108 amino acids of the p62 subunit of TFIIH make up a pleckstrin homology and phosphotyrosine binding (PH/PTB) domain that specifically interacts with XPG (50). This PH/PTB domain is not required for transcription or the integrity of TFIIH and NMR studies showed that it forms a defined 3D structure, providing a first glimpse of a modular domain involved in the interaction between TFIIH and XPG. An important future challenge will be to further determine the molecular basis of the interaction of various modules of TFIIH and XPG.

ACKNOWLEDGEMENTS

We are grateful to J.M. Egly and O. Nikaido for gifts of antibodies. This work was supported by the Swiss National Science Foundation (grant No. 3100A0-100487 and the "Frontiers in Genetics" NCCR program to SGC and grants No. 3100A0-00744 and 3130-054873 to ODS), and New York State Office of Science and Technology and Academic Research (NYSTAR) grant No. C040069 to ODS. Funding to pay the Open Access publication charge was provided by the Swiss National Science Foundation.

Conflict of interest statement. None declared.

REFERENCES

- Lieber, M.R. (1997) The FEN-1 family of structure-specific nucleases in eukaryotic DNA replication, recombination and repair. *Bioessays*, **19**, 233–240.
- Liu, Y., Kao, H.I. and Bambara, R.A. (2004) Flap endonuclease 1: a central component of DNA metabolism. *Annu. Rev. Biochem.*, **73**, 589–615.
- Henneke, G., Friedrich-Heineken, E. and Hubscher, U. (2003) Flap endonuclease 1: a novel tumour suppressor protein. *Trends Biochem. Sci.*, **28**, 384–390.
- Gillet, L.C. and Schärer, O.D. (2006) Molecular mechanisms of mammalian global genome nucleotide excision repair. *Chem. Rev.*, **106**, 253–276.
- Friedberg, E.C., Walker, G.C., Siede, W., Wood, R.D., Schultz, R.A. and Ellenberger, T. (2005) *DNA Repair and Mutagenesis*, 2nd edn. ASM Press, Washington, DC.
- Clarkson, S.G. (2003) The XPG story. *Biochimie*, **85**, 1113–1121.
- O'Donovan, A., Davies, A.A., Moggs, J.G., West, S.C. and Wood, R.D. (1994) XPG endonuclease makes the 3' incision in human DNA nucleotide excision repair. *Nature*, **371**, 432–435.
- Evans, E., Fellows, J., Coffer, A. and Wood, R.D. (1997) Open complex formation around a lesion during nucleotide excision repair provides a structure for cleavage by human XPG protein. *EMBO J.*, **16**, 625–638.

9. Wakasugi, M., Reardon, J.T. and Sancar, A. (1997) The non-catalytic function of XPG protein during dual incision in human nucleotide excision repair. *J. Biol. Chem.*, **272**, 16030–16034.
10. Mu, D., Wakasugi, M., Hsu, D.S. and Sancar, A. (1997) Characterization of reaction intermediates of human excision repair nuclease. *J. Biol. Chem.*, **272**, 28971–28979.
11. Constantinou, A., Gunz, D., Evans, E., Lalle, P., Bates, P.A., Wood, R.D. and Clarkson, S.G. (1999) Conserved residues of human XPG protein important for nuclease activity and function in nucleotide excision repair. *J. Biol. Chem.*, **274**, 5637–5648.
12. Cloud, K.G., Shen, B., Strniste, G.F. and Park, M.S. (1995) XPG protein has a structure-specific endonuclease activity. *Mutat. Res.*, **347**, 55–60.
13. Hohl, M., Thorel, F., Clarkson, S.G. and Schärer, O.D. (2003) Structural determinants for substrate binding and catalysis by the structure-specific endonuclease XPG. *J. Biol. Chem.*, **278**, 19500–19508.
14. Robins, P., Pappin, D.J., Wood, R.D. and Lindahl, T. (1994) Structural and functional homology between mammalian DNase IV and the 5'-nuclease domain of Escherichia coli DNA polymerase I. *J. Biol. Chem.*, **269**, 28535–28538.
15. Murante, R.S., Rust, L. and Bambara, R.A. (1995) Calf 5' to 3' exo/endonuclease must slide from a 5' end of the substrate to perform structure-specific cleavage. *J. Biol. Chem.*, **270**, 30377–30383.
16. Harrington, J.J. and Lieber, M.R. (1995) DNA structural elements required for FEN-1 binding. *J. Biol. Chem.*, **270**, 4503–4508.
17. Kao, H.I., Henricksen, L.A., Liu, Y. and Bambara, R.A. (2002) Cleavage specificity of Saccharomyces cerevisiae flap endonuclease 1 suggests a double-flap structure as the cellular substrate. *J. Biol. Chem.*, **277**, 14379–14389.
18. Xie, Y., Liu, Y., Argueso, J.L., Henricksen, L.A., Kao, H.I., Bambara, R.A. and Alani, E. (2001) Identification of rad27 mutations that confer differential defects in mutation avoidance, repeat tract instability, and flap cleavage. *Mol. Cell. Biol.*, **21**, 4889–4899.
19. Ceska, T.A., Sayers, J.R., Stier, G. and Suck, D. (1996) A helical arch allowing single-stranded DNA to thread through T5 5'-exonuclease. *Nature*, **382**, 90–93.
20. Mueser, T.C., Nossal, N.G. and Hyde, C.C. (1996) Structure of bacteriophage T4 RNase H, a 5' to 3' RNA-DNA and DNA-DNA exonuclease with sequence similarity to the RAD2 family of eukaryotic proteins. *Cell*, **85**, 1101–1112.
21. Hosfield, D.J., Mol, C.D., Shen, B. and Tainer, J.A. (1998) Structure of the DNA repair and replication endonuclease and exonuclease FEN-1: coupling DNA and PCNA binding to FEN-1 activity. *Cell*, **95**, 135–146.
22. Hwang, K.Y., Baek, K., Kim, H.Y. and Cho, Y. (1998) The crystal structure of flap endonuclease-1 from Methanococcus jannaschii. *Nat. Struct. Biol.*, **5**, 707–713.
23. Storic, F., Henneke, G., Ferrari, E., Gordenin, D.A., Hübscher, U. and Resnick, M.A. (2002) The flexible loop of human FEN1 endonuclease is required for flap cleavage during DNA replication and repair. *EMBO J.*, **21**, 5930–5942.
24. Chapados, B.R., Hosfield, D.J., Han, S., Qiu, J., Yelent, B., Shen, B. and Tainer, J.A. (2004) Structural basis for FEN-1 substrate specificity and PCNA-mediated activation in DNA replication and repair. *Cell*, **116**, 39–50.
25. Friedrich-Heineken, E. and Hübscher, U. (2004) The Fen1 extrahelical 3'-flap pocket is conserved from archaea to human and regulates DNA substrate specificity. *Nucleic Acids Res.*, **32**, 2520–2528.
26. Scherly, D., Nospikel, T., Corlet, J., Ucla, C., Bairoch, A. and Clarkson, S.G. (1993) Complementation of the DNA repair defect in xeroderma pigmentosum group G cells by a human cDNA related to yeast RAD2. *Nature*, **363**, 182–185.
27. Iyer, N., Reagan, M.S., Wu, K.J., Canagarajah, B. and Friedberg, E.C. (1996) Interactions involving the human RNA polymerase II transcription/nucleotide excision repair complex TFIIH, the nucleotide excision repair protein XPG, and Cockayne syndrome group B (CSB) protein. *Biochemistry*, **35**, 2157–2167.
28. He, Z., Henricksen, L.A., Wold, M.S. and Ingles, C.J. (1995) RPA involvement in the damage-recognition and incision steps of nucleotide excision repair. *Nature*, **374**, 566–569.
29. Volker, M., Mone, M.J., Karmakar, P., van Hoffen, A., Schul, W., Vermeulen, W., Hoeijmakers, J.H., van Driel, R., van Zeeland, A.A. *et al.* (2001) Sequential assembly of the nucleotide excision repair factors *in vivo*. *Mol. Cell*, **8**, 213–224.
30. Araujo, S.J., Nigg, E.A. and Wood, R.D. (2001) Strong functional interactions of TFIIH with XPC and XPG in human DNA nucleotide excision repair, without a preassembled repairosome. *Mol. Cell. Biol.*, **21**, 2281–2291.
31. Riedl, T., Hanaoka, F. and Egly, J.M. (2003) The comings and goings of nucleotide excision repair factors on damaged DNA. *EMBO J.*, **22**, 5293–5303.
32. Dunand-Sauthier, I., Hohl, M., Thorel, F., Jaquier-Gubler, P., Clarkson, S.G. and Schärer, O.D. (2005) The spacer region of XPG mediates recruitment to nucleotide excision repair complexes and determines substrate specificity. *J. Biol. Chem.*, **280**, 7030–7037.
33. Thorel, F., Constantinou, A., Dunand-Sauthier, I., Nospikel, T., Lalle, P., Raams, A., Jaspers, N.G., Vermeulen, W., Shivji, M.K. *et al.* (2004) Definition of a short region of XPG necessary for TFIIH interaction and stable recruitment to sites of UV damage. *Mol. Cell. Biol.*, **24**, 10670–10680.
34. Moggs, J.G., Yarema, K.J., Essigmann, J.M. and Wood, R.D. (1996) Analysis of incision sites produced by human cell extracts and purified proteins during nucleotide excision repair of a 1,3-intrastrand d(GpTpG)-cisplatin adduct. *J. Biol. Chem.*, **271**, 7177–7186.
35. Ellison, A.R., Nospikel, T., Jaspers, N.G., Clarkson, S.G. and Gruenert, D.C. (1998) Complementation of transformed fibroblasts from patients with combined xeroderma pigmentosum-Cockayne syndrome. *Exp. Cell Res.*, **243**, 22–28.
36. Biggerstaff, M. and Wood, R.D. (1999) Assay for nucleotide excision repair protein activity using fractionated cell extracts and UV-damaged plasmid DNA. *Methods Mol. Biol.*, **113**, 357–372.
37. Moriwaki, S., Stefanini, M., Lehmann, A.R., Hoeijmakers, J.H., Robbins, J.H., Rapin, I., Botta, E., Tanganelli, B., Vermeulen, W. *et al.* (1996) DNA repair and ultraviolet mutagenesis in cells from a new patient with xeroderma pigmentosum group G and cockayne syndrome resemble xeroderma pigmentosum cells. *J. Invest. Dermatol.*, **107**, 647–653.
38. Okinaka, R.T., Perez-Castro, A.V., Sena, A., Laubscher, K., Strniste, G.F., Park, M.S., Hernandez, R., MacInnes, M.A. and Kraemer, K.H. (1997) Heritable genetic alterations in a xeroderma pigmentosum group G/Cockayne syndrome pedigree. *Mutat. Res.*, **385**, 107–114.
39. Clement, V., Dunand-Sauthier, I. and Clarkson, S.G. (2006) Suppression of UV-induced apoptosis by the human DNA repair protein XPG. *Cell Death Differ.*, **13**, 478–488.
40. Harrington, J.J. and Lieber, M.R. (1994) The characterization of a mammalian DNA structure-specific endonuclease. *EMBO J.*, **13**, 1235–1246.
41. Kim, C.Y., Park, M.S. and Dyer, R.B. (2001) Human flap endonuclease-1: conformational change upon binding to the flap DNA substrate and location of the Mg²⁺ binding site. *Biochemistry*, **40**, 3208–3214.
42. Friedrich-Heineken, E., Henneke, G., Ferrari, E. and Hübscher, U. (2003) The acetyltable lysines of human Fen1 are important for endo- and exonuclease activities. *J. Mol. Biol.*, **328**, 73–84.
43. Mori, T., Nakane, M., Hattori, T., Matsunaga, T., Ihara, M. and Nikaïdo, O. (1991) Simultaneous establishment of monoclonal antibodies specific for either cyclobutane pyrimidine dimer or (6-4)photoproduct from the same mouse immunized with ultraviolet-irradiated DNA. *Photochem. Photobiol.*, **54**, 225–232.
44. Smit, N.P., Vink, A.A., Kolb, R.M., Steenwinkel, M.J., van den Berg, P.T., van Nieuwpoort, F., Roza, L. and Pavel, S. (2001) Melanin offers protection against induction of cyclobutane pyrimidine dimers and 6-4 photoproducts by UVB in cultured human melanocytes. *Photochem. Photobiol.*, **74**, 424–430.
45. Katsumi, S., Kobayashi, N., Imoto, K., Nakagawa, A., Yamashina, Y., Muramatsu, T., Shirai, T., Miyagawa, S., Sugiura, S. *et al.* (2001) In situ visualization of ultraviolet-light-induced DNA damage repair in locally irradiated human fibroblasts. *J. Invest. Dermatol.*, **117**, 1156–1161.
46. Sarker, A.H., Tsutakawa, S.E., Kostek, S., Ng, C., Shin, D.S., Peris, M., Campeau, E., Tainer, J.A., Nogales, E. *et al.* (2005) Recognition of RNA polymerase II and transcription bubbles by XPG, CSB, and TFIIH: insights for transcription-coupled repair and Cockayne Syndrome. *Mol. Cell*, **20**, 187–198.

47. Mone, M.J., Volker, M., Nikaido, O., Mullenders, L.H., van Zeeland, A.A., Verschure, P.J., Manders, E.M. and van Driel, R. (2001) Local UV-induced DNA damage in cell nuclei results in local transcription inhibition. *EMBO Rep.*, **2**, 1013–1017.
48. Houtsmuller, A.B., Rademakers, S., Nigg, A.L., Hoogstraten, D., Hoeijmakers, J.H. and Vermeulen, W. (1999) Action of DNA repair endonuclease ERCC1/XPF in living cells. *Science*, **284**, 958–961.
49. Stauffer, M.E. and Chazin, W.J. (2004) Structural mechanisms of DNA replication, repair, and recombination. *J. Biol. Chem.*, **279**, 30915–30918.
50. Gervais, V., Lamour, V., Jawhari, A., Frindel, F., Wasielewski, E., Dubaele, S., Egly, J.M., Thierry, J.C., Kieffer, B. *et al.* (2004) TFIIH contains a PH domain involved in DNA nucleotide excision repair. *Nat. Struct. Mol. Biol.*, **11**, 616–622.